Consistent Estimation of Cardiac Motions by 4D Image Registration

Dinggang Shen, Hari Sundar, Zhong Xue, Yong Fan, and Harold Litt

Section of Biomedical Image Analysis, Department of Radiology,
University of Pennsylvania, Philadelphia, PA 19104
Dinggang.Shen@uphs.upenn.edu

Abstract. A 4D image registration method is proposed for consistent estimation of cardiac motion from MR image sequences. Under this 4D registration framework, all 3D cardiac images taken at different time-points are registered simultaneously, and motion estimated is enforced to be spatiotemporally smooth, thereby overcoming potential limitations of some methods that typically estimate cardiac deformation sequentially from one frame to another, instead of treating the entire set of images as a 4D volume. To facilitate our image matching process, an attribute vector is designed for each point in the image to include intensity, boundary and geometric moment invariants (GMIs). Hierarchical registration of two image sequences is achieved by using the most distinctive points for initial registration of two sequences and gradually adding less-distinctive points for refinement of registration. Experimental results on real data demonstrate good performance of the proposed method in registering cardiac images and estimating motions from cardiac image sequences.

1 Introduction

Heart attack, stroke and other cardiovascular diseases have been the leading cause of death since 1919 [1]. Importantly, cardiovascular disease kills more Americans than the next seven causes combined, including cancer. Cardiac imaging techniques were developed for providing qualitative and quantitative information about the morphology and function of the heart [2]. In particular, spatiotemporal imaging is a valuable tool for understanding cardiac motion and perfusion, and their relationship with the stages of disease. For assisting the diagnosis and treatment of cardiac diseases, automated methods are needed to analyze a large set of cardiac images and to extract clinically relevant parameters.

Cardiac motion estimation is an important step for quantification of the elasticity and contractility properties of the myocardium, related to the regional function of heart. In the setting of ischemic heart disease, localized regions with abnormal motion are related to the existence of infarcted or hibernating segments, the function of which has been affected by insufficient tissue microcirculation. Extensive research has shown that regional function measures, i.e., wall-thickening, strain, and torsion, may be earlier sub-clinical markers for examining left ventricular dysfunction and myocardial diseases, although ventricular mass, volume, and ejection fraction are considered as a standard for evaluating global function of heart [3].

J. Duncan and G. Gerig (Eds.): MICCAI 2005, LNCS 3750, pp. 902 – 910, 2005.

Many motion estimation methods have been developed for quantification of the deformation of regional myocardial tissue, and they fall into three categories. *The first category* of methods tracks invasive or noninvasive markers in cardiac images. Implanting invasive markers into the myocardium tends to influence the regional motion pattern of the wall muscle. Accordingly, MR tagging was developed to provide noninvasive mathematical markers inside the myocardium, which can deform with myocardial motion [4]. MR imaging and especially tagged MR are currently the reference modalities to estimate dense cardiac displacement fields with high spatial resolution. The deformation fields, as well as the derived motion parameters such as myocardial strain, can be determined with accuracy [5,6]. *The second category* of methods uses segmentation of the myocardial wall, followed by geometrical and mechanical modeling using active contours or surfaces to extract the displacement field and to perform the motion analysis [5,7,8]. For matching two contours or surfaces, curvatures are frequently used to establish initial sparse correspondences, followed by the dense correspondence interpolation in other myocardial positions by regularization or mechanical modeling [5,9]. *The third category* of methods uses energy-based warping or optical flow techniques to compute the displacement of the myocardium [10-12]. There also exists a method taking advantages of *both* the second *and* the third categories, i.e., tracking the cardiac boundaries by image curvatures [13]. Recently, 4D models are also proposed for cardiac registration and segmentation [14,15,16].

We propose a 4D deformable registration method for consistent motion estimation from 3D cardiac image sequences. The main premise of the proposed method is that, if suitable attribute vectors can be designed to serve as morphological signatures for distinctive points in a cardiac image sequence, then by hierarchically matching those attribute vectors along with appropriate regularization we can yield an accurate estimation of cardiac motion. Also, by integrating all temporal cardiac images into a single 4D registration framework, it is possible to estimate temporally consistent cardiac motion, since the constraints of temporal smoothness and consistency can be performed concurrently with the image registration procedure.

2 Method

2.1 Formulating Motion Estimation as Image Registration

Cardiac motion estimation is a problem of finding a transformation to describe how each point **x** in the heart moves over the time *t*. If each point **x** in the image at a certain time-point can be related to its corresponding position in the images at other time-points by an image registration method, cardiac motion can be immediately estimated. Thus, for estimating cardiac motion from end-diastole to other times in a periodic sequence of N 3D images, i.e., $I(\mathrm{x},t)=\{I_t,1\le t\le N\}$ with I_1 as an end-diastolic image, we need only to register end-diastolic image I_1 to images at other time-points.

In order to use a 4D image registration for simultaneously estimating the motion from the end-diastolic image I_1 to all other time-points $\{I_t\}$, we generate a new 4D image, i.e., a new image sequence $T(\mathbf{x},t)=\{I_1,...,I_1\}$, which repeats the end-diastolic image I_1 as images at N different time-points (Fig 1). Thus, by registering the 4D

images $I(\mathbf{x},t)$ to $T(\mathbf{x},t)$ via a spatial transformation $h(\mathbf{x},t)$, we can estimate motion for each point $\mathbf{x}$ in the end-diastolic I_1 to all other time-points in a cardiac sequence. Notably, the transformation $h(\mathbf{x},t)$ is restricted to 3D spatial deformations at the same time-point, since no temporal differences exist in the generated image sequence $T(\mathbf{x},t)$ and thus no need to consider temporal variations.

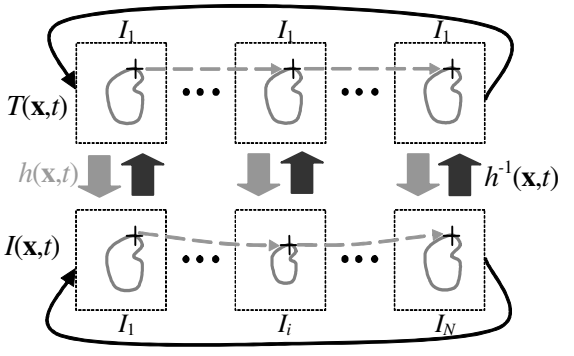

Fig. 1. Formulation of cardiac motion estimation as a 4D image registration problem

2.2 Attribute Vector

In order to register two image sequences accurately, we design for each point a morphological signature, i.e., an attribute vector $\mathbf{a}(\mathbf{x},t)$, for the purpose of minimizing the ambiguity in image matching and correspondence detection during the deformable registration procedure. Each attribute vector includes not only image intensity, but also boundary and Geometric Moment Invariants (GMIs) [17], all of which are computed from the 3D spatial images. For generated image sequence $T(\mathbf{x},t)$, we need only to compute attribute vectors for one 3D image and other identical images just take the same set of attribute vectors. GMIs are computed from different neighborhood sizes, and are concatenated into a long attribute vector. GMIs at a particular scale are calculated by placing a spherical neighborhood around each voxel and calculating a number of parameters that are invariant to rotation. The detailed definitions for attribute vectors and their similarities are the same as in [17].

2.3 Energy Function

The 4D image registration is completed by hierarchically matching attribute vectors in the two image sequences. To make the registration independent of which of the two sequences is treated as the template [18,17], the energy that evaluates the match of two image sequences should be symmetrically designed for two image sequences under registration. That means, both the forward transformation $h(\mathbf{x},t)$ and backward transformation $h^{-1}(\mathbf{x},t)$ should be evaluated in a single energy function, and forced to be consistent with each other.

To allow the registration algorithm to focus on different sets of image points adaptively during different stages of image registration, each point should have its own energy term and the whole energy function should be a weighted summation of all

points' energy terms. Therefore, by hierarchically assigning those weights according to the distinctiveness of attribute vectors, i.e., assigning large weights for the energy terms of the points with distinctive attribute vectors (such as points with high curvatures along the left ventricular border) and zero weights for the energy terms of other points, we can focus on the most suitable points to actively drive the image registration. Effectively, this procedure approximates what would be a very high-dimensional (equal to the number of points in the two image sequences) cost function, by a significantly lower-dimensional function of only the active points. This latter function has few local minima, because it is a function of the coordinates of active points, for which relatively unambiguous matches can be found. Therefore, using this strategy, we can speed up the performance of image registration and also reduce the chances of local minima, which in part result from ambiguities in determining the matching pairs of points.

Also, the transformation $h(\mathbf{x},t)$ should be smooth spatially and temporally. Since the image sequences are periodic, i.e., the first image I_1 and the last image I_N are also temporal neighbors as indicated by solid arrows in Fig 1, the temporal smoothness constraint should be applied between the first and the last images in the periodic sequence. In this way, after completing 4D image registration, it is ensured that each point $\mathbf{x}$ moves smoothly along the temporal direction from the end-diastolic image I_1 to other time-points, and importantly moves back to its original position since the first images respectively in the two sequences are identical and transformation between them is thus forced to be exactly zero during the entire registration procedure.

By considering all of above-described requirements, the energy function that our 4D registration algorithm minimizes is defined as follows:

$$E = E_F + E_B + E_C + E_S,$$

where

$$E_F = \sum_{t=1}^{N} \sum_{\mathbf{x}} \omega_T(\mathbf{x},t) \left(\sum_{(\mathbf{z},\tau)\in n(\mathbf{x},t)} d\left(\mathbf{a}_T(\mathbf{z},\tau), \mathbf{a}_I(h(\mathbf{z},\tau))\right) \right)$$

$$E_B = \sum_{t=1}^{N} \sum_{\mathbf{x}} \omega_I(\mathbf{x},t) \left(\sum_{(\mathbf{z},\tau)\in n(\mathbf{x},t)} d\left(\mathbf{a}_T(h^{-1}(\mathbf{z},\tau)), \mathbf{a}_I(\mathbf{z},\tau)\right) \right)$$

$$E_C = \sum_{t=1}^{N} \sum_{\mathbf{x}} \varepsilon_T(\mathbf{x},t) \left(\sum_{(\mathbf{z},\tau)\in n(\mathbf{x},t),\ t\neq\tau} d\left(\mathbf{a}_I(h(\mathbf{z},t)), \mathbf{a}_I(h(\mathbf{z},\tau))\right) \right)$$

$$E_S = \alpha \cdot E_S^{\text{Spatial}} + \beta \cdot E_S^{\text{Temporal}}$$

There are four energy terms in this energy function. The first term E_F is defined on the forward transformation $h(\mathbf{x},t)$, and measures the similarity of attribute vectors between each point in the sequence $T(\mathbf{x},t)$ and its corresponding one in the sequence $I(\mathbf{x},t)$. The second energy term E_B is similar to the first term, while it is defined on the inverse transformation $h^{-1}(\mathbf{x},t)$ to make sure that each point in the sequence $I(\mathbf{x},t)$ also finds its best matching point in the sequence $T(\mathbf{x},t)$. Specifically, in the first energy term, the importance of each point $(\mathbf{x},t)$ in the image registration is determined by its corresponding parameter $\omega_T(\mathbf{x},t)$, which is designed to be proportional

to the distinctiveness of this point's attribute vector $\mathbf{a}_T(\mathbf{x},t)$. The match for each point $(\mathbf{x},t)$ is evaluated in its 4D (3D spatial and 1D temporal) neighborhood $n(\mathbf{x},t)$, by integrating all differences between the attribute vector $\mathbf{a}_T(\mathbf{z},\tau)$ of every neighboring point $(\mathbf{z},\tau)$ and the attribute vector $\mathbf{a}_I(h(\mathbf{z},\tau))$ of the corresponding point $h(\mathbf{z},\tau)$ in the sequence $I(\mathbf{x},t)$. The difference of two attribute vectors $d(\cdot,\cdot)$ ranges from 0 to 1 [17]. The size of neighborhood $n(\mathbf{x},t)$ is large initially and decreases gradually with the progress of the deformation, thereby increasing robustness and accuracy of deformable registration.

The third energy term E_C measures the attribute-vector matching of corresponding points in different time-point images of the sequence $I(\mathbf{x},t)$. Notably, for each point $(\mathbf{x},t)$ in the sequence $T(\mathbf{x},t)$, its corresponding point in the sequence $I(\mathbf{x},t)$ is $h(\mathbf{x},t)$. Since the sequence $T(\mathbf{x},t)$ has identical images at different time-points, i.e., same end-diastolic image, points $\{(\mathbf{x},t),1 \le t \le N\}$ are N corresponding points in the sequence $T(\mathbf{x},t)$; accordingly, N transformed points $\{h(\mathbf{x},t),1 \le t \le N\}$ are the established correspondences in the sequence $I(\mathbf{x},t)$. In this way, we can require the attribute vector $\mathbf{a}_I(h(\mathbf{x},t))$ of a point $h(\mathbf{x},t)$ in the image $I(\mathbf{x},t)$ be similar to the attribute vector $\mathbf{a}_I(h(\mathbf{x},\tau))$ of its corresponding point $h(\mathbf{x},\tau)$ in the neighboring time-point image $I(\mathbf{x},\tau)$. This requirement is repeated for each position $(\mathbf{z},\tau)$ in a 4D neighborhood $n(\mathbf{x},t)$, and the total attribute-vector difference is weighted by $\varepsilon_T(\mathbf{x},t)$ to reflect the importance of a point $(\mathbf{x},t)$ in the sequence $T(\mathbf{x},t)$. The use of this energy term potentially makes it easier to solve the 4D registration problem, since the registration of cardiac images of neighboring time-points is relatively easier and thus it can provide a good initialization for 4D image registration by initially focusing only on energy terms of E_c and E_S.

The fourth energy term E_S is a smoothness constraint for the transformation $h(\mathbf{x},t)$. For convenience, we separate this smoothness constraint into two components, i.e., a spatial smoothness constraint E_S^{Spatial} and a temporal smoothness constraint E_S^{Temporal}, and these two constraints are linearly combined by their own weighting parameters α and β. For the *spatial* smoothness constraint, we use a Laplacian operator [17] to impose spatial smoothness. Notably, all images in the sequence $T(\mathbf{x},t)$ are identically the end-diastolic image. Thus, for registering two image sequences $T(\mathbf{x},t)$ and $I(\mathbf{x},t)$, we have to register the end-diastolic image with the end-systolic image by a large nonlinear transformation, which might be over-smoothed by the Laplacian operator. To avoid this over-smoothing problem, we use a multi-resolution framework, i.e., multi-level transformations, to implement our registration algorithm. Each resolution will estimate its own level of transformation based on the total transformations estimated from the previous resolutions, and the final transformation used to register two image sequences is the summation of all levels of transformations respectively estimated from all resolutions. Notably, the Laplacian operator is only allowed to smooth the current level of transformation being estimated in the *current resolution*, which effectively avoids smoothing the transformations estimated from the previous resolutions. As for the *temporal* smoothness constraint, we use a Gaussian filter to obtain an average transformation in a 1D temporal neighborhood around each point $(\mathbf{x},t)$, and force the transformation on this point $(\mathbf{x},t)$ to follow its average transformation in temporal neighborhood.

3 Results

The first experiment is designed to show the performance of the proposed method in estimating cardiac motion and deformation fields. There are 33 different time-point images in total, taken from a cardiac cycle of a normal volunteer, with the first time-point at end-diastole. Some selected cardiac images are shown in Fig 2(a). With the transformations established between end-diastolic frame and other frames, we can warp the end-diastolic image to any of the other frames, as shown in Fig 2(b), which becomes very similar to the corresponding frame, partly indicating the accuracy of our registration algorithm. Also, from Fig 2(c) that shows the deformation fields around the left ventricle at end-diastole to other time-points, we can observe that the deformation fields are very smooth in each time-point, and consistent over time.

The accuracy of motion and deformation estimation can also be reflected by the performance of the boundary tracking/labeling results provided by the 4D registration method. For example, if the boundaries of interest have been labeled in the end-diastolic image, we can warp these labeled boundaries to other time-points and obtain the boundary tracking/labeling results at other time-points. Fig 3 shows our semi-automatically labeled boundaries of interest as red contours in two images with black borders, respectively called long-axis and short-axis views at end-diastole. The tracking/labeling results at other time-points are shown by red contours in other images in Figs 3(a) and 3(b). Moreover, we can display the temporal views of short-axis lines to

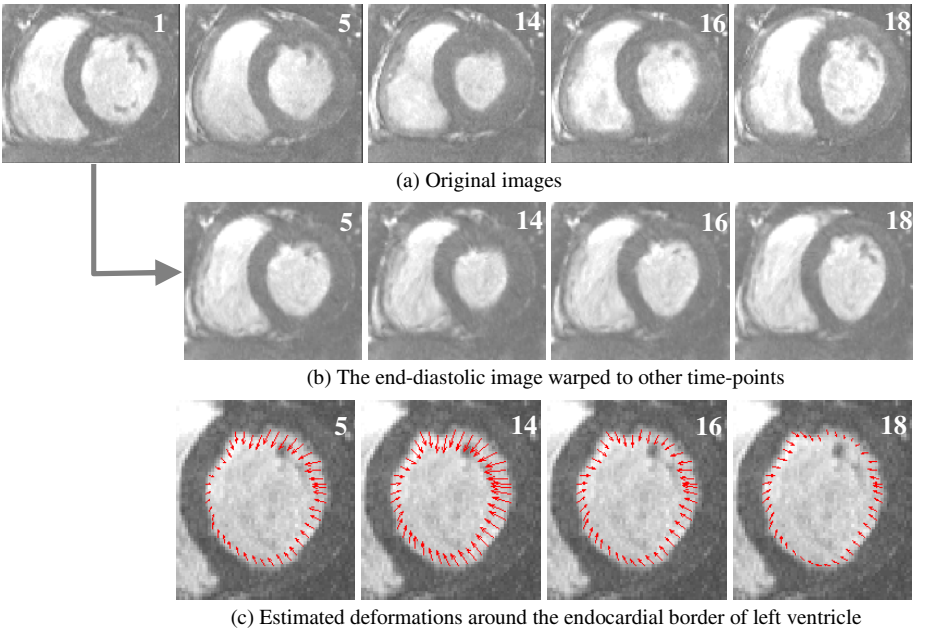

Fig. 2. Estimating deformations from end-diastole to other time-points. (a) 5 selected cardiac images, (b) the results of warping end-diastole to other time-points, (c) deformations around left ventricle, estimated from the end-diastolic image and cropped here for clear display.

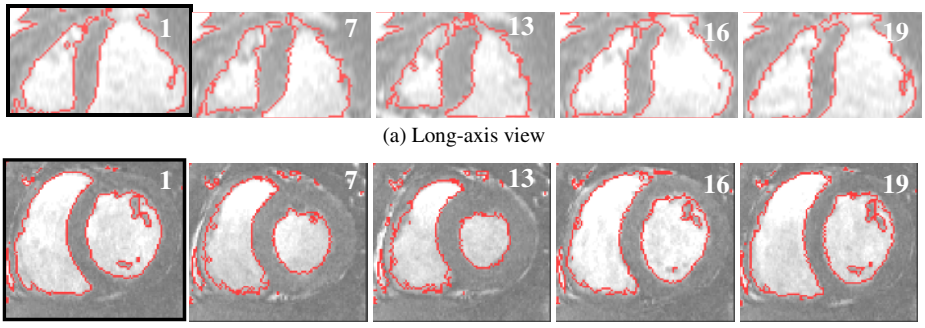

Fig. 3. Tracking/labeling the boundaries of interest in a cardiac sequence

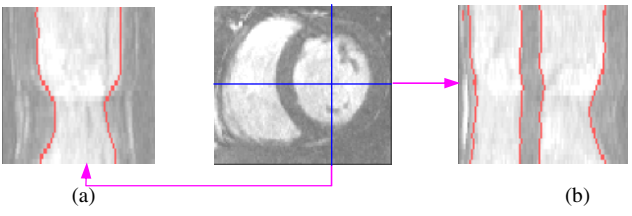

Fig. 4. Tracking/labeling results in temporal views of two short-axis lines. The red colors indicate the labeling results on the left and right ventricular boundaries.

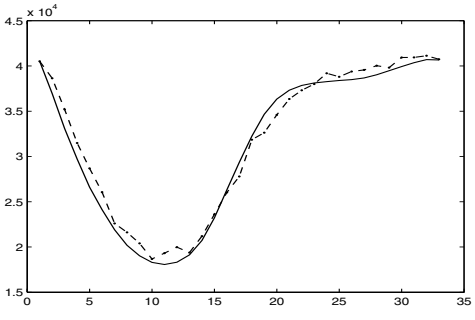

Fig. 5. Left ventricular volume of a selected subject, segmented by our algorithm (solid curve) and by hand (dotted curve) over all frames in a cardiac cycle

show the temporal tracking/labeling results. As shown in Fig 4, the proposed algorithm is able to track/label the two short-axis lines over time.

We also validated our method on a small dataset of 3D cardiac image sequences, by comparing the left-ventricular volumes obtained respectively by manual and automatic segmentations. Average volume error is 3.37%, with standard deviation 2.56%; and average volume overlap error is 7.04%, with standard deviation 3.28%. Correlation coefficient between manual and automatic segmentations is 0.99. Fig 5 shows the comparison on a selected subject over a whole cardiac cycle.

4 Conclusion

We have presented a 4D deformable registration method for estimation of cardiac motions from MR image sequences. The experimental results show consistent motion estimation by our method. This performance is achieved by formulating the cardiac motion estimation as a 4D image registration problem, which simultaneously considers all images of different time-points and further constrains the spatiotemporal smoothness of estimated motion fields concurrently with the image registration procedure. Also, compared to other motion estimation methods that use very simple features such as curvature of the left ventricular border, our method uses a rich set of attributes, including GMIs, to distinguish the corresponding points across different time-points, thereby maximally reducing ambiguity in image matching. Finally, by hierarchically selecting the active points to match, based on the distinctiveness degrees of their attribute vectors, our registration algorithm has more opportunities to produce a global solution for motion estimation.

Our 4D registration method for cardiac applications needs extensive validation in the future, by using both simulated and real data. For simulated data, we will validate the accuracy of our registration algorithm by directly comparing our estimated motions with ground-truth motions that we simulate. For real data, we will compare the algorithm-detected correspondences with the manually placed correspondences in the different frames, in order to validate the motions estimated.

References

1. American Heart Association, 1999. [Online]. Available: http://www.americanheart.org.
2. A.F. Frangi, W.J. Niessen, M.A. Viergever, "Three-Dimensional Modeling for Functional Analysis of Cardiac Images: A Review", *IEEE Trans. Med. Img.*, 20(1): 1-25, Jan 2001.
3. L. Pan, J. A. C. Lima, N.F. Osman, "Fast Tracking of Cardiac Motion Using 3D-HARP", *IPMI'2003*, pp. 611-622.
4. E.A. Zerhouni, D.M. Parish, W.J. Rogers, A. Yang, and E.P. Shapiro, "Human heart: tagging with MR imaging - a method for noninvasive assessment of myocardial motion", *Radiology*, 169(1): 59-63, 1988.
5. P. Shi, A. J. Sinusas, R.T. Constable, and J.S. Duncan, "Volumetric deformation analysis using mechanics-based data fusion: applications in cardiac motion recovery", *International Journal of Computer Vision*, vol. 35, no. 1, pp. 87–107, 1999.
6. J.L. Prince and E.R. McVeigh, "Motion Estimation From Tagged MR Image Sequences", *IEEE Trans. Medical Imaging*, 11(2):238-249, June 1992.
7. X. Papademetris, A.J. Sinusas, D.P. Dione and J.S. Duncan, "Estimation of 3D Left Ventricular Deformation from Echocardiography". *Medical Image Analysis*, 5:17-28, 2001.
8. Y. Wang, Yasheng Chen, and Amir A. Amini, "Fast LV motion estimation using subspace approximation", *IEEE Transactions on Medical Imaging*, Vol. 20, pp. 499-513, 2001.
9. McEachen, II, J.C., Nehorai, A., Duncan, J.S., "Multiframe Temporal Estimation of Cardiac Nonrigid Motion", *IEEE Trans. Image Processing*, 9(4):651-665, April 2000.
10. M.J. Ledesma-Carbayo, J. Kybic, M. Desco, A. Santos, M. Unser, "Cardiac Motion Analysis from Ultrasound Sequences Using Non-Rigid Registration", *MICCAI'01*, pp. 889-896, Utrecht, The Netherlands, October 14-17, 2001.

11. S. Song and R. Leahy, “Computation of 3D velocity fields from 3D cine CT images of a human heart”, *IEEE Trans. Med. Imag*, Vol. MI-10, pp 295-306, Sep 1991.
12. R. Chandrashekara, D. Rueckert, R. Mohiaddin, “Cardiac Motion Tracking in Tagged MR Images Using a 4D B-spline Motion Model and Nonrigid Image Registration”, *ISBI* 2004: 468-471.
13. N. Lin, X. Papademetris, J.S. Duncan, “Analysis of Left Ventricular Motion Using a General Robust Point Matching Algorithm”, *MICCAI*, pp. 556-563, 2003.
14. D. Perperidis, R. Mohiaddin, D. Rueckert, “Spatio-Temporal Free-Form Registration of Cardiac MR Image Sequences”, *MICCAI*, pp.911-919, 2004.
15. J. Montagnat, H. Delingette, “4D Deformable Models with temporal constraints: application to 4D cardiac image segmentation”, *Med. Image Analysis*, 9(1):87-100, Feb 2005.
16. J. Declerck, J. Feldmar, and N. Ayache, “Definition of a 4D continuous planispheric transformation for the tracking and the analysis of left-ventricle motion,” *Medical Image Analysis*, vol. 2, no. 2, pp. 197-213, 1998.
17. D. Shen, C. Davatzikos, “HAMMER: Hierarchical Attribute Matching Mechanism for Elastic Registration”, *IEEE Trans. on Medical Imaging*, 21(11):1421-1439, Nov 2002.
18. G.E. Christensen and H.J. Johnson, “Consistent Image Registration”, *IEEE TMI*, 20(7), 2001, pp. 568-582.